New Mechanistic Insight into the Coupling Reactions of CO_2 and Epoxides in the Presence of Zinc Complexes

Hoon Sik Kim,*[a] Jai Jun Kim,[a, b] Sang Deuk Lee,[a] Myoung Soo Lah,[c] Dohyun Moon,[c] and Ho Gyeom Jang*[b]

Abstract: Coupling reactions of CO_2 and epoxide to produce cyclic carbonates were performed in the presence of a catalyst $[L_2ZnX_2]$ (L = pyridine or substituted pyridine; X = Cl, Br, I), and the effects of pyridine and halide ligands on the catalytic activity were investigated. The catalysts with electron-donating substituents on pyridine ligands exhibit higher activity than those with unsubstituted pyridine ligands. On the other hand, the catalysts with electron-withdrawing substituents at the 2-position of the pyridine ligands show no activity; this demonstrates the importance of the basicity of the pyridine ligands. The catalytic activity of $[L_2ZnX_2]$ was found to decrease with increasing electronegativity of the halide ligands. A series of highly active zinc complexes bridged by pyridinium alkoxy ions of the general formula $[\{(\mu\text{-}OCHRCH_2L)ZnBr_2\}_n]$ ($n = 2$ for $R = CH_3$; $n = 3$ for $R = H$; L = pyridine or substituted pyridine) were synthesized and characterized by X-ray crystallography. The dinuclear zinc complexes obtained from propylene oxide adopt a square-planar geometry for the Zn_2O_2 core with two bridging pyridinium propoxy ion ligands. Trinuclear zinc complexes prepared from ethylene oxide adopt a boat geometry for the Zn_3O_3 core, in which three zinc and three oxygen atoms are arranged in an alternate fashion. These zinc complexes bridged by pyridinium alkoxy ions were also isolated from the coupling reactions of CO_2 and epoxides performed in the presence of $[L_2ZnBr_2]$. Rapid CO_2 insertion into the zinc–oxygen bond of the zinc complexes bridged by pyridinium alkoxy ions leads to the formation of zinc carbonate species; these which yield cyclic carbonates and zinc complexes bridged by pyridinium alkoxy ions upon interaction with epoxides. The mechanistic pathways for the formation of active species and cyclic carbonates are discussed on the basis of results from structural and spectroscopic analyses.

Keywords: alkylene carbonate · carbon dioxide fixation · epoxides · green chemistry · homogeneous catalysis

Introduction

The transformation of CO_2 into cyclic carbonates by the coupling reaction with epoxides [Eq. (1)] has received much attention with regard to the utilization of CO_2, a gas responsible for global warming.[1, 2]

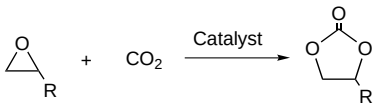

(1)

[a] Dr. H. S. Kim, J. J. Kim, Dr. S. D. Lee
CFC Alternatives Research Center, KIST
39-1, Hawolgokdong, Seongbukgu Seoul 136-791 (Korea)
Fax: (+82) 2-958-5859
E-mail: khs@kist.re.kr

[b] Prof. Dr. H. G. Jang, J. J. Kim
Division of Chemistry and Molecular Engineering
Korea University, Seoul 136-130 (Korea)

[c] Prof. Dr. M. S. Lah, D. Moon
Department of Applied Chemistry and Chemistry
College of Science and Technology, Hanyang University
1271 Sa-1-dong, Ansan, Kyunggi-do 425-791 (Korea)

Five-membered cyclic carbonates are solvents that can be used in many different application areas including polyurethanes, oils, paints, resins, in foundries, and in the entire life-science market segment.[3] In addition, cyclic carbonates are used as raw materials in a wide range of chemical reactions: the production of ethylene glycol esters, hydroxyalkyl derivatives, carbamates, alkylene sulfides, polyurethanes, polyesters, and polycarbonates.[4, 5] Recently, there has been an increasing demand for cyclic carbonates for use in secondary and fuel-cell batteries and as solvents for polymer and gel electrolytes.[6, 7]

Accordingly, a substantial amount of literature has been published on catalyst development and mechanisms for the coupling reactions.[8–10] The use of transition-metal/halide catalysts along with *tert*-alkylammonium halides or alkali-metal halides has been shown to be a highly active combination for promoting the coupling reactions in which the halide ligands act as nucleophiles.[11–14] The reactivity pattern of these catalytic systems suggest that an epoxide is coordinated to the halogenated metal anion, generated from the interaction of the metal halide with the halide ion, and the resulting

0947-6539/03/0903-0678 $ 20.00+.50/0

coordinated epoxide ring is opened by the halide ion to form an haloalkoxy species.[13, 14] Nucleophilic attack of the haloalkoxy species on CO_2 leads to a linear halocarbonate that is transformed into a cyclic carbonate by the intramolecular substitution of the halide.

The catalytic systems composed of transition-metal halides ($AlCl_3$, $NiCl_2$, $MoCl_5$, etc.) and Lewis bases such as amines or phosphines have also been employed in the selective formation of cyclic carbonates under mild conditions.[15]

Recently, Mg and Mg–Al mixed oxides with strong basic sites on their surface have been shown to effectively catalyze this coupling reaction. Catalysis has been explained based on results from surface characterization of catalysts by using physicochemical methods.[16]

Zinc(II) complexes have also been used as catalysts, because of their high activity in the cyclization and copolymerization of CO_2 and epoxides.[17–20] However, despite the intensive studies on the reaction mechanism,[21, 22] active species or potential intermediates to clarify the reaction pathway for the formation of cyclic carbonates have never been structurally characterized or isolated. During the course of our studies on the development of active catalysts and on the mechanism for the coupling reaction of CO_2 and epoxides, we have found that $[L_2ZnX_2]$ complexes (L = pyridine or substituted pyridine; X = Cl, Br, I), prepared from ZnX_2 and L, are highly active for the coupling reaction. Furthermore, we have isolated an active species, dinuclear zinc bromide complexes with two bridging pyridinium alkoxy ligands, $[Zn_2Br_4(\mu\text{-}OCHCH_3CH_2\text{-}NC_5H_5)_2]$, from the coupling reaction of CO_2 and propylene oxide performed in the presence of $[(C_5H_5N)_2ZnBr_2]$.[23] To gain deeper understanding of the reaction pathway and to elucidate the role of the Lewis base more clearly, we have conducted mechanistic studies on the coupling reactions in the presence of a well-defined soluble catalyst **1** $[L_2ZnBr_2]$ (**1a**: L = pyridine, **1b**: L = 2-methylpyridine, **1c**: L = 4-methyl pyridine, **1d**: L = 4-*tert*-butylpyridine, **1e**: L = 2-chloropyridine, **1f**: L = 2-acetylpyridine, **1g** = 2,2′-dipyridyl, **1h** = 4-dimethylaminopyridine).

Herein, we report the syntheses, characterization and reactivities of a series of active zinc complexes of the general formula $[\{(\mu\text{-}OCHRCH_2L)ZnBr_2\}_n]$ ($n = 2$ for $R = CH_3$; $n = 3$ for R = H; L = pyridine or substituted pyridine) thatclearly demonstrate the reaction pathway for the formation of cyclic carbonates and the role of the pyridine ligand in the formation of active species.

Results and Discussion

In the course of our studies on the mechanistic aspects of the coupling reaction, we have succeeded in isolating an active intermediate species (**2a-PO**) from the coupling reaction of CO_2 with propylene oxide performed at 100 °C and 3.4 MPa for 1 h in the presence of **1a**.

To our surprise, ^{1}H NMR spectroscopy and single-crystal X-ray diffraction studies revealed that the intermediate species is a dinuclear zinc complex containing two pyridinium alkoxo adducts that bridge to the two electrophilic zinc centers (Figure 1). As described in the Experimental Section,

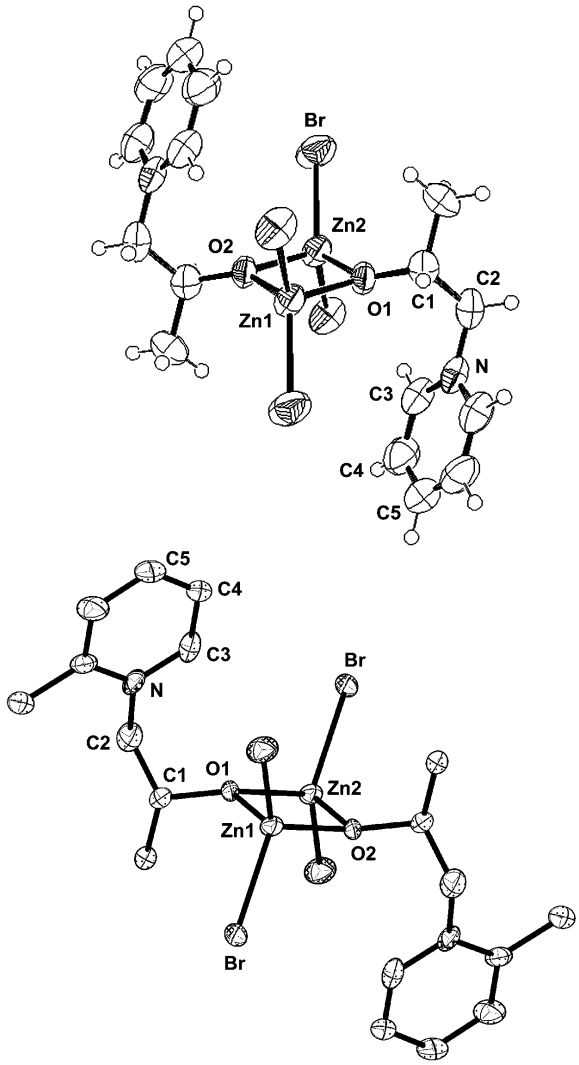

Figure 1. Molecular structures of complexes **2a-PO** (top) and **2b-PO** (bottom) showing the atom labeling scheme.

the dinuclear complex **2a-PO** has also been prepared in high yield from the reaction of **1a** with propylene oxide in CH_2Cl_2 in the absence of CO_2. Another dinuclear zinc complex, **2b-PO**, has been similarly prepared by reacting propylene oxide with the corresponding substituted pyridine. Interestingly, the reaction of **1a–c** with ethylene oxide leads to the formation of the trinuclear zinc complexes **2a-EO**, **2b-EO**, and **2c-EO**, respectively. The aggregation state of the zinc complexes seems to be largely influenced by the methyl substitution on the epoxide moiety, but independent of the methyl substitution on the pyridine ring. Such an aggregation of zinc alkoxides has previously been observed and well studied by van Koten et al.[24–26]

The structural analysis of these dinuclear and trinuclear zinc complexes shows that both pyridine ligands in $[L_2ZnBr_2]$ are dissociated from the zinc center. The coordination of an epoxide is likely to take place by substituting one of the pyridine ligands, which in turn attacks on the electropositive carbon atom of the coordinated epoxide to produce a pyridinium alkoxy ion species.

  0947-6539/03/0903-0679 $ 20.00+.50/0

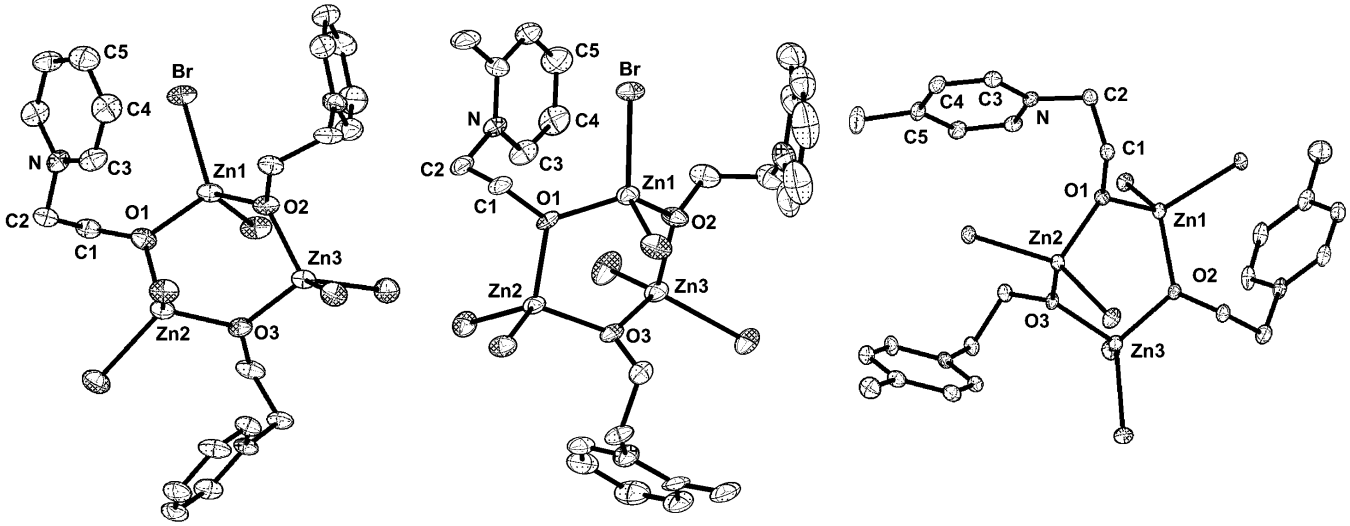

Figure 2. Molecular structures of complexes **2a-EO** (left), **2b-EO** (middle), and **2c-EO** (right) showing the atom labeling scheme.

Complexes **2a-PO** and **2b-PO** (Figure 1) and **2a-EO**, **2b-EO**, and **2c-EO** (Figure 2) have been characterized by X-ray crystallography. A list of selected bond lengths and angles is provided in Table 1. Dinuclear zinc complexes **2a-PO** and **2b-PO** adopt a square-planar geometry for the Zn_2O_2 core with two bridging propoxy ligands between the two zinc centers.

Table 1. Selected bond lengths [Å] and bond angles [°] for complexes **2a-PO**, **2b-PO**, **2a-EO**, **2b-EO**, and **2c-EO**.

	2a-PO dimer	**2b-PO** dimer	**2a-EO** trimer	**2b-EO** trimer	**2c-EO** trimer
Zn1–O1	1.956(5)	1.973(5)	1.977(5)	1.964(5)	1.963(2)
Zn1–O2	1.971(5)	1.977(5)	1.964(5)	1.962(5)	1.966(2)
Zn1–Br1	2.338(2)	2.373(2)	2.381(1)	2.393(1)	2.401(6)
O1–C1	1.424(10)	1.426(9)	1.414(9)	1.428(8)	1.420(3)
C1–C2	1.495(13)	1.531(13)	1.525(11)	1.494(11)	1.528(4)
C2–N1	1.477(12)	1.471(12)	1.494(10)	1.486(9)	1.468(4)
N1–C3	1.321(11)	1.345(11)	1.341(10)	1.347(9)	1.360(4)
C3–C4	1.353(14)	1.462(18)	1.360(12)	1.373(12)	1.364(5)
C4–C5	1.365(14)	1.34(2)	1.378(13)	1.368(13)	1.394(5)
O1-Zn1-O2	83.0(2)	83.8(2)	104.2(2)	104.8(2)	107.85(9)
Zn1-O1-Zn2	97.0(2)	96.2(2)	114.9(3)	117.3(2)	115.2(1)
Br1-Zn1-Br2	110.86(6)	113.89(5)	114.28(5)	110.94(5)	113.24(2)

Even though **2a-PO** and **2b-PO** are prepared from racemic propylene oxide, they exist as only *R*, *S*-diastereomeric dimers in the crystal structures due to the presence of centers of symmetry. Accordingly, *R*,*R* and *S*,*S* diastereomers are not observed. Trinuclear zinc complexes **2a-EO**, **2b-EO**, and **2c-EO** adopt a boat geometry for the Zn_3O_3 core; in which three zinc and three oxygen atoms are alternately arranged. Each zinc center in these di- and trinuclear complexes has a distorted tetrahedral geometry. The Zn–O bond lengths in these di- and trinuclear zinc complexes are in the range from 1.954 to 1.978 Å, and are comparable to those found in previously reported zinc alkoxide and phenoxide complexes (1.864 to 2.061 Å).[24–29]

The structures of di- and trinuclear zinc complexes reveal various important aspects of zinc-catalyzed coupling reactions of epoxides and CO_2 such as ligand (pyridine) dissociation, coordination of epoxides, and ring opening of Lewis acids activated epoxides by Lewis bases (dissociated pyridine) through the formation of a pyridinium adduct. Ring opening of epoxides seems to occur exclusively at the less sterically hindered carbon atom.[30, 31]

The insertion of CO_2 into the metal–oxygen bond of alkoxides or phenoxides is well established,[32, 33] and, therefore, we have tested the reaction of **2a-PO** with CO_2 to observe the formation of zinc carbonate species.

The reaction of complex **2a-PO** with 0.14 MPa of CO_2 in DMSO at 25 °C for 3 h produced an unknown compound, **3a-PO**. The formation of **3a-PO** was monitored by FTIR spectroscopy under 0.21 MPa of CO_2 as described in the experimental section. Figure 3 shows that two peaks at 1326

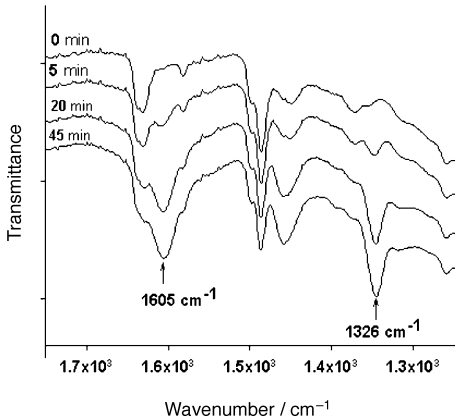

Figure 3. FTIR spectra for the interaction of complex **2a-PO** with CO_2.

and 1605 cm^{-1}, corresponding to the metal carbonate, increase gradually with time, confirming the formation of a zinc carbonate species.[34, 35] The interaction of CO_2 with **2a-PO** was also confirmed by ^1H and ^{13}C NMR studies. Upon introduction of $^{13}CO_2$ into a NMR tube containing **2a-PO** in [D_6]DMSO, a new set of broad resonances appears in the ^1H NMR spectrum (Figure 4B). The newly appeared broad resonances in the aromatic ($\delta = 8.0 - 9.0$ ppm) and propylene

0947-6539/03/0903-0680 $ 20.00+.50/0 *Chem. Eur. J.* **2003**, *9*, No. 3

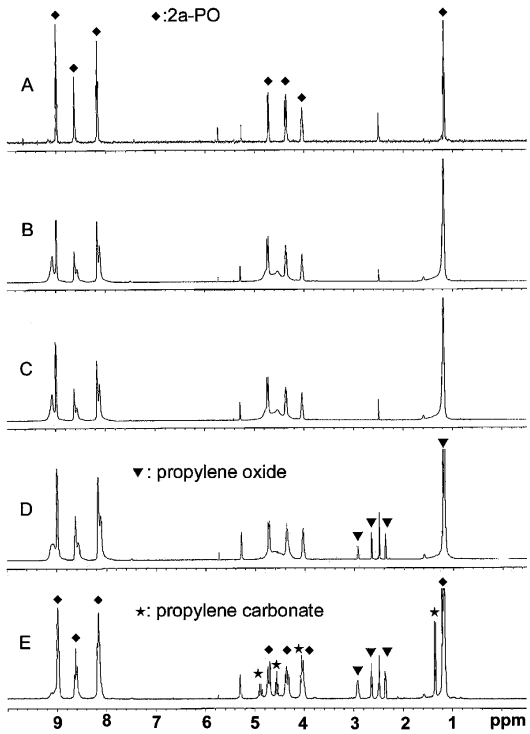

Figure 4. ^1H NMR spectra: A) **2a-PO** in [D_6]DMSO; B) after introduction of 0.14 MPa of $^{13}CO_2$ into A); C) after degassing of B); D) after addition of propylene oxide to C); E) after reaction of D) at 80 °C for 30 min.

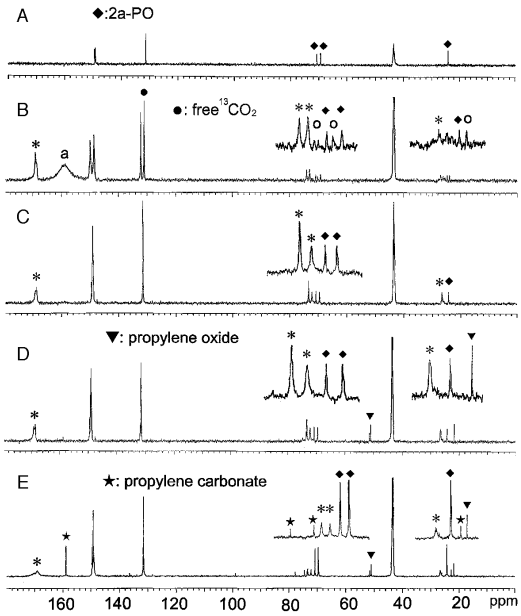

Figure 5. ^{13}C NMR spectra: A) **2a-PO** in [D_6]DMSO; B) after introduction of 0.14 MPa of $^{13}CO_2$ into A); C) after degassing of B); D) after addition of propylene oxide to C); E) after reaction of D) at 80 °C for 30 min.

oxide moiety region ($\delta = 4.0-5.0$, 1.0–1.2 ppm) are likely to be associated with formation of zinc carbonate species. After removal of free $^{13}CO_2$ under vacuum (Figure 4C), the NMR tube was charged with propylene oxide and heated at 80 °C for 30 min. As expected, propylene carbonate was produced and most of the zinc carbonate species disappeared (see Figure 4D and E), indicating that the carbonate species are the intermediates for the formation of cyclic carbonates. This can be more clearly seen in ^{13}C NMR spectra in Figure 5. As can be seen in Figure 5B, the introduction of 0.14 MPa of $^{13}CO_2$ into the NMR tube containing **2a-PO** in [D_6]DMSO results in the formation of a zinc carbonate species with the sacrifice of **2a-PO** (◆). When the sample (B) was degassed under vacuum to remove free $^{13}CO_2$, the peak at $\delta = 128$ ppm for free $^{13}CO_2$ and a broad peak centered at 158 ppm in the carbonyl region (a), and associated small peaks at 20–80 ppm (○) completely disappeared. It is likely that **2a-PO** reversibly interacts with CO_2 to form a very unstable CO_2-coordinated zinc species, which in turn transforms into the zinc carbonate species, **3a-PO**. The evacuated sample (Figure 5C) clearly shows the characteristic carbonate resonance at $\delta = 170$ ppm along with the small peaks (*) corresponding to the propylene moiety connected to the carbonate group. When propylene oxide (▼) was treated with a sample (C) containing the carbonate species **3a-PO** at 80 °C for 30 min, ^{13}C-labeled propylene carbonate (★) was produced and **2a-PO** was regenerated (see Figure 5D and E). The regeneration of **2a-PO** from **3a-PO** can be clearly seen from the comparison of their peak intensities. From the regeneration of **2a-PO** from **3a-PO** and the formation of ^{13}C-labeled propylene carbonate, manifested by the strong intensity of the carbonyl peak for the propylene carbonate at $\delta = 159$ ppm, it is evident that the zinc carbonate species **3a-PO** is an important intermediate for the formation of propylene carbonate.

Attempts to obtain a single crystal of compound **3a-PO** for X-ray crystallographic analysis failed, but based on the above spectroscopic results compound **3a-PO** is assumed to have a structure similar to **2a-PO**.

The activities of various zinc complexes containing pyridine or substituted pyridine ligands have been tested for the coupling reactions of epoxides with CO_2. The results are shown in Table 2.

Table 2. Catalytic activities of various catalysts for the coupling reactions of CO_2 and epoxides.[a]

Entry	Catalysts	TOF[b] [h^{-1}] PO	EO
1	Pyridine (Py)	n.r.[c]	n.r.
2	$ZnBr_2$	n.r.	n.r.
3	[Py_2ZnCl_2]	38	170
4	[Py_2ZnBr_2] (**1a**)	308	890
5	[Py_2ZnI_2]	420	980
6	[(2-CH_3-Py)$_2$$ZnBr_2$] (**1b**)	435	1216
7	[(4-CH_3-Py)$_2$$ZnBr_2$] (**1c**)	350	980
8	[(4-*tert*-butyl-Py)$_2$$ZnBr_2$] (**1d**)	364	755
9	[(2-Cl-Py)$_2$$ZnBr_2$] (**1e**)	tr.[d]	tr.
10	[(2-CH_3CO-Py)$_2$$ZnBr_2$] (**1f**)	tr.	tr.
11	[(2,2′-dipyridyl)$ZnBr_2$] (**1g**)	n.r.	n.r.
12	[(4-dimethylaminopyridine)$_2$$ZnBr_2$] (**1h**)	516	1060
13	**2a-EO**	327	1180
14	**2a-PO**	340	1200
15	**2b-PO**	530	1450

[a] Reaction conditions: $T = 100$ °C, p (CO_2) = 3.4 MPa, reaction time 1 h for EO and 2 h for PO, molar ratios : EO/Zn = 1500, PO/Zn = 1000. [b] TOF = turnover frequency (moles of cyclic carbonate produced per mole of zinc per hour). PO = propylene oxide, EO = ethylene oxide. [c] n.r. = no reaction. [d] tr. = trace.

Substitution on the pyridine ligand in **1** is found to have a striking effect on the catalytic activity for the coupling reaction between CO_2 and epoxides. The catalyst containing electron-donating alkyl-substituted pyridine ligands, **1b**, **1c** or **1d** exhibits a higher activity relative to **1a**. On the other hand, the catalyst containing pyridine ligands with an electron-withdrawing chlorine or acetyl group at the 2-position (**1e**, **1f**), shows very little catalytic activity.

The basicity of pyridine ligands with an electron-donating group is higher than those with an electron-withdrawing group, and, therefore, the Zn–N bond strength in $[L_2ZnBr_2]$ would be weaker for the less basic pyridine ligand. If the major role of the pyridine ligands in **1** is to provide coordination sites for an incoming epoxide by being dissociated from the zinc center, the catalyst containing less-basic (less-nucleophilic) pyridine ligands should exhibit higher activity than the catalyst with electron-donating alkyl-substituted pyridine ligands. In contrast, the catalysts with less-basic pyridine ligands such as 2-chloro- and 2-acetylpyridine show very little activity, suggesting the importance of nucleophilicity of the pyridine ligand. This is confirmed from the enhanced activity of the zinc complex containing the highly nucleophilic 4-dimethylaminopyridine (**1h**). However, ligand dissociation should also be considered as an important factor in determining the catalytic activity, since the zinc complexe containing a strongly chelating 2,2′-dipyridyl ligand (**1g**) shows no activity for the coupling reactions.

The effect of added pyridine was investigated and the results are listed in Table 3. The catalytic activity decreases with increasing amount of added pyridine, implying that the pyridine attack on the complexed epoxide is not a rate-determining step. The coordination of an epoxide to form an active species seems to be somewhat prevented by the presence of added pyridine. In other words, epoxide and added pyridine compete with each other for coordination to the zinc center.

Table 3. Effect of added pyridine on the catalytic activity for the coupling reaction of CO_2 and ethylene oxide.[a]

Entry	Catalyst	Added pyridine	TOF [h^{-1}]
1	$[Py_2ZnBr_2]$	0 equiv[b]	890
2	$[Py_2ZnBr_2]$	1 equiv	753
3	$[Py_2ZnBr_2]$	3 equiv	486
4	$[Py_2ZnBr_2]$	5 equiv	382

[a] Reaction conditions: $T = 100\,^{\circ}C$, $p(CO_2) = 3.4$ MPa, reaction time 1 h, molar ratio: EO/Zn = 1500, [b] Number of molar equivalents to catalyst.

From the activity test and the structural characterization of the zinc complexes bridged by pyridinium alkoxy ions, it is likely that the major role of the pyridine ligands is the ring opening of the coordinated epoxide. This would form an active species through a nucleophilic attack on the electropositive carbon atom of the epoxide. Therefore, the stronger the basicity of the pyridine ligand, the easier the ring opening of the coordinated epoxide. In fact, the inactive catalysts, **1e** and **1f** did not react with the epoxide to produce the corresponding zinc complexes bridged by pyridinium alkoxy ions, even at 80 °C for 10 h, supporting the above explanation.

It is interesting to note that the activities of the pyridinium alkoxy ion bridged complexes **2** are higher than those of the corresponding precursors, **1**. These results can be attributed to the presence of an induction period for the formation of active species (**2**) from their precursors. The effect of solubility of catalysts on the catalytic activity has not been considered because **2** is much less soluble than **1** in the reaction media.

To have a better understanding of the active species and the mechanistic pathway for the formation of cyclic carbonates, we carried out a series ^1H NMR experiments with **2a-PO** and **2a-EO**.

As shown in Figure 6, complex **2a-PO** was found to retain its integrity even after the coupling reaction of CO_2 with propylene oxide performed at 100 °C under 3.4 MPa of CO_2 for 1 h. Likewise, complex **2a-EO** was isolated unchanged

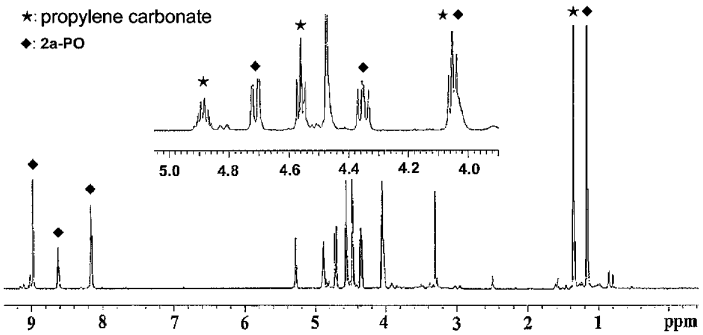

Figure 6. ^1H NMR spectra of complex **2a-PO** recovered after the coupling reaction of CO_2 with propylene oxide performed at 100 °C under 3.4 MPa of CO_2 for 1 h.

from the reaction of CO_2 and ethylene oxide in the presence of complex **2a-EO**. These results strongly suggest that pyridinium alkoxy ion bridged complexes are the active species. The possibility of the interconversion between **2a-PO** and **2a-EO** through an epoxide exchange was investigated by carrying out the coupling reaction of CO_2 and ethylene oxide at 100 °C and 3.4 MPa for 1 h. However, the ^1H NMR spectra of the product mixtures shown in Figure 7 indicate that the epoxide exchange is not taking place during catalysis [Eq. (2)].

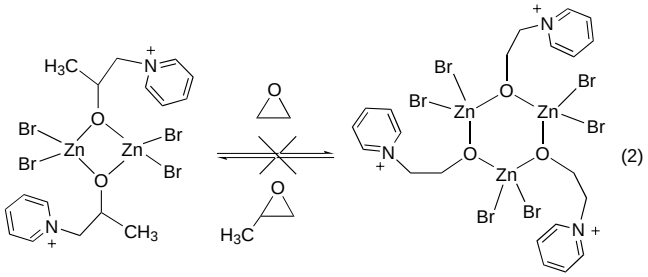

The pyridine exchange reaction, through a C–N bond cleavage in the bridging pyridinium alkoxy ligands, was also examined by conducting the coupling reaction of CO_2 and propylene oxide in the presence of **2a-PO** and 2-methylpyridine at 100 °C (molar ratio of 2-methylpyridine/**2a-PO** = 3). Characterization of the product mixture by ^1H NMR spectros-

0947-6539/03/0903-0682 $ 20.00+.50/0 *Chem. Eur. J.* **2003**, *9*, No. 3

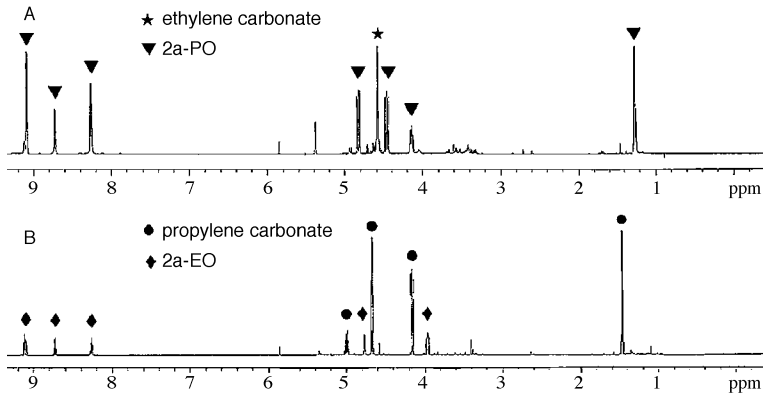

Figure 7. ^{1}H NMR spectra of complex **2a-PO** and **2a-EO** recovered after the coupling reaction of CO_2 with epoxides performed at 100 °C under 3.4 MPa of CO_2 for 1 h. A) catalyst = **2a-PO**, epoxide = ethylene oxide; B) catalyst = **2a-EO**, epoxide = propylene oxide.

copy showed that the reaction of **2a-PO** with 2-methylpyridine to give **2b-PO** does not take place. It is likely that the displacement of pyridine on an alkoxy pyridinium by another pyridine is an extremely slow process due to the high activation-energy barrier.

The halide ligands have been considered as nucleophiles to open the coordinated epoxide ring in most of the metal–halide-catalyzed coupling reactions.[13, 14] However, the halide ligands in complex **1** seem to play a role in controlling the dissociation of pyridine ligands and not in the ring opening of the epoxide as nucleophiles. This is somewhat supported by the experimental results in Table 2. The activity of **1** decreases with increasing electronegativity of the halide ligand for the coupling reaction of CO_2 and propylene oxide. The substitution of pyridine ligands by an incoming epoxide would be more difficult for the catalyst with more electronegative halide ligands due to the increased Zn–N bond strength.

On the basis of the activity test and the mechanistic studies described above, a reasonable mechanism for the coupling reaction of epoxide and CO_2 can be proposed, and is shown in Scheme 1.

The initial coordination of the epoxide by replacing one of the pyridine ligands is likely to occur first. Nucleophilic attack of the dissociated pyridine on the less sterically hindered carbon atom of the coordinated epoxide and the subsequent dimerization of the resulting pyridinium alkoxy ion species lead to the formation of active species **2**. The insertion of CO_2 into the Zn–O bond of **2** would give a carbonate-bridged intermediate **3**. The coordination of an additional epoxide to **3** followed by the elimination of a cyclic carbonate can generate **2**. However, the possibility that **2** or **3** exists as monomeric species under experimental conditions cannot be completely ruled out.

The structure of **2a-PO** in [D_7]DMF (m.p. $-$-61 °C) was studied by variable temperature NMR spectroscopy to see if monomeric species are present in solution, and if so, to determine the equilibrium between dimeric and monomeric zinc species (Scheme 2). The ^{1}H NMR spectrum of **2a-PO**, compared to that recorded at ambient temperature, remains unchanged even when recorded at -55 °C. This may imply that the equilibrium is too fast to observe in this temperature range, or only one species, either dimer or monomer, exists in solution. No evidence is found for the absence of monomeric species in solution by this NMR experiment. Cryoscopic molecular weight determination was employed to unambiguously determine the degree of association of **2** in solution. This failed due to the extremely low solubility of di- and trinuclear zinc alkoxide complexes.

Efforts to obtain a crystal structure of **3a-PO** and to find the aggregation states of **2** and **3** in solution are in progress. This should provide better understanding of the mechanism of the coupling reactions between CO_2 and epoxides.

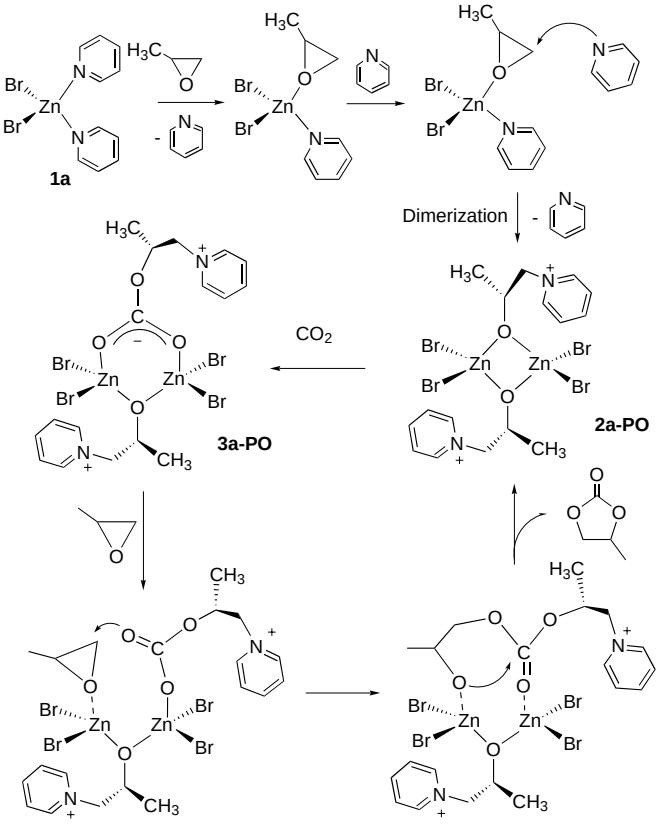

Scheme 1. Proposed mechanism for the coupling reaction of CO_2 and propylene oxide in the presence of **1a**.

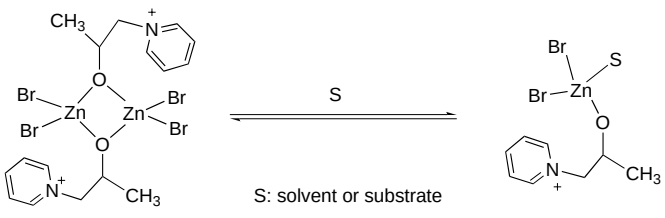

Scheme 2. Possible monomer-dimer equilibrium of **2a** in solution.

Conclusion

Coupling reactions of CO_2 and epoxides to produce cyclic carbonates have been performed in the presence of a catalyst $[L_2ZnX_2]$ (L = pyridine or substituted pyridine; X = Cl, Br, I). The effects of pyridine and halide ligands on the catalytic activity and the formation of active species have been investigated. The catalysts with electron-donating substituents on pyridine ligands exhibit higher activity than those with unsubstituted pyridine ligands. On the other hand, the catalysts with electron-withdrawing substituents on pyridine ligands show no activity; this demonstrates the importance of the nucleophilicity of the pyridine ligands. A zinc complex containing a strongly chelating 2,2′-dipyridyl ligand (**1g**) was found to be totally inactive, indicating that ligand dissociation is also an important factor in the catalysis process.

Unlike the most of metal–halide-catalyzed coupling reactions, halide ions in **1** are found to play a role in controlling the dissociation of the pyridine ligand, but not in the ring opening of epoxides as nucleophiles. The catalytic activity of $[L_2ZnX_2]$ is found to decrease with increasing electronegativity of the halide ligands. A series of di- and trinuclear zinc complexes with bridging pyridinium alkoxy ion ligands have been synthesized from the reactions of $[L_2ZnX_2]$ and epoxides with or without the presence of CO_2. The structural characterization of these complexes by X-ray crystallography clearly demonstrates the role of the pyridine ligands in the formation of active species in the coupling reactions of CO_2 with epoxides performed in the presence of $[L_2ZnX_2]$. The aggregation state of these complexes is likely to be largely determined by the kind of epoxide, not by the pyridine ligand in $[L_2ZnX_2]$: dinuclear zinc complexes are formed with propylene oxide and trinuclear zinc complexes with ethylene oxide. The dinuclear zinc complexes adopt a square-planar geometry of the Zn_2O_2 core with two bridging pyridinium propoxy ion ligands, while trinuclear zinc complexes adopt a boat geometry for the Zn_3O_3 core with three bridging pyridinium alkoxy ion ligands. These di- and trinuclear zinc complexes show higher activities for the coupling reactions of CO_2 and epoxides than the corresponding precursors $[L_2ZnBr_2]$, indicating the presence of an induction period. NMR and FTIR experiments showed that zinc complexes bridged by pyridinium alkoxy ions rapidly interact with CO_2 to give zinc carbonate species, which in turn react with additional epoxides to generate further bridged zinc complexes and cyclic carbonates. Pyridine exchange through a C–N bond cleavage in the pyridinium alkoxy ion ligands and the structural transformation between di- and trinuclear complexes have not been observed during the coupling reactions. This suggests that zinc complexes bridged by pyridinium alkoxy ions are the active species in the catalysis.

Experimental Section

Method and materials: All manipulations were carried out under argon unless otherwise stated, with glassware thatwas flame-dried prior to use. The solvents were freshly distilled before use according to literature procedures. Ethylene oxide was purchased from Hyundai Petrochemical Co. and used as received. Propylene oxide was purchased from Aldrich Chemical Co. and used without further purification. Pyridine, 2-methylpyridine, 3-methylpyridine, 4-methylpyridine, 2,2′-dipyridyl, 4-dimethylaminopyridine, $ZnCl_2$, and ZnI_2 were purchased from Aldrich Chemical Co. $ZnBr_2$ was purchased from Fluka Chemical Co. CO_2 and $^{13}CO_2$ were purchased from Sin Yang Gas Co. and Aldrich Chemical Co., respectively. $[L_2ZnX_2]$ (X: Cl, Br, I; L = pyridine or substituted pyridine) was prepared according to the published procedure.[36] IR spectra were recorded on a Mattson Infinity Spectrometer with MCT detector. ^1H and ^{13}C NMR spectra were recorded on a Varian Unity 600 superconducting high-resolution spectrometer. Elemental analysis was carried out by the Advanced Analytical Center at KIST using a Perkin–Elmer 2400 CHNS analyzer.

Synthesis of $[Zn_2Br_4\{\mu\text{-}OCH(CH_3)CH_2\text{-}NC_5H_5\}_2]$ (2a-PO): A solution of **1a** (2.00 g, 5.22 mmol) in methylene chloride (30 mL) was treated with propylene oxide (0.50 mL, 7.15 mmol) in a 60 mL high-pressure glass reactor and stored at room temperature for 10 h. The precipitate was filtered onto a glass filter and dried under vacuum to give a white solid. Yield: 85%; elemental analysis calcd (%) for $C_{16}H_{22}Br_4N_2O_2Zn_2$: C 26.52, H 3.06, Br 44.10, N 3.87, Zn 18.04; found: C 25.90, H 2.95, N 3.79, Zn 19.51; ^1H NMR (600 MHz, [D$_6$]DMSO, 25 °C): $\delta = 1.20$ (d, $^2J(H,H) = 6$ Hz, 3H; CH_3), 4.04 (m, 1H; CH), 4.36 (dd, $^2J(H,H) = 13$ Hz, 1H; CH_2), 4.73 (dd, $^2J(H,H) = 13$ Hz, 1H; CH_2), 8.15 (t, $^3J(H,H) = 6$ Hz, 2H; C_5H_5N), 8.61 (t, $^3J(H,H) = 8$ Hz, 1H; C_5H_5N), 8.97 ppm (d, $^2J(H,H) = 6$ Hz, 2H; C_5H_5N).

Synthesis of $[Zn_2Br_4\{\mu\text{-}OCH(CH_3)CH_2\text{-}NC_5H_4(2\text{-}CH_3)\}_2]$ (2b-PO): Complex **2b-PO** was prepared in a manner similar to that employed in the preparation of **2a-PO** by simply replacing **1a** with **1b**. Yield: 70%; elemental analysis calcd (%) for $C_{18}H_{26}Br_4N_2O_2Zn_2$: C 28.72, H 3.48, Br 42.46, N 3.72, Zn 17.37; found: C 28.70, H 3.65, N 3.73, Zn 17.41; ^1H NMR (600 MHz, [D$_6$]DMSO, 25 °C): $\delta = 1.20$ (d, $^2J(H,H) = 6$ Hz, 3H; CH_3), 2.80 (s, 3H; CH_3), 4.03 (m, 1H; CH), 4.37 (dd, $^2J(H,H) = 12$ Hz, 1H; CH_2), 4.71 (dd, $^2J(H,H) = 13$ Hz, 1H; CH_2), 8.13 (t, $^3J(H,H) = 7$ Hz, 1H; C_5H_5N), 8.19 (d, $^2J(H,H) = 8$ Hz, 1H; C_5H_5N), 8.64 (t, $^3J(H,H) = 6$ Hz, 1H; C_5H_5N), 8.98 ppm (d, $^2J(H,H) = 6$ Hz, 1H; C_5H_5N).

Synthesis of $[Zn_3Br_6(\mu\text{-}OCH_2CH_2\text{-}NC_5H_5)_3]$ (2a-EO): Complex **2a-EO** was prepared in a manner analogous to that described above for complex **2a-PO** by replacing propylene oxide with ethylene oxide. Yield: 87%; elemental analysis calcd (%) for $C_{21}H_{27}Br_6N_3O_3Zn_3$: C 24.14, H 2.60, Br 45.88, N 4.02, Zn 18.77; found: C 23.52, H 2.57, N 3.92, Zn 17.54; ^1H NMR (600 MHz, [D$_6$]DMSO, 25 °C): $\delta = 3.90$ (t, $^3J(H,H) = 5$ Hz, 2H; CH_2), 4.71 (t, $^3J(H,H) = 5$ Hz, 2H; CH_2), 8.20 (t, $^3J(H,H) = 7$ Hz, 2H; C_5H_5N), 8.66 (t, $^3J(H,H) = 8$ Hz, 1H; C_5H_5N), 9.05 ppm (d, $^2J(H,H) = 6$ Hz, 2H; C_5H_5N).

Synthesis of $[Zn_3Br_6\{\mu\text{-}OCH_2CH_2\text{-}NC_5H_4(2\text{-}CH_3)\}_3]$ (2b-EO): This complex was prepared in a manner analogous to that described above for complex **2a-EO** by simply replacing **1a** with **1b**. Yield: 78%; elemental analysis calcd (%) for $C_{24}H_{33}Br_6N_3O_3Zn_3$: C 26.52, H 3.06, Br 44.10, N 3.87, Zn 18.04; found: C 26.02, H 3.00, N 3.73, Zn 17.52; ^1H NMR (600 MHz, [D$_6$]DMSO, 25 °C): $\delta = 2.96$ (s, 3H; CH_3), 3.96 (t, $^3J(H,H) = 6$ Hz, 2H; CH_2), 4.75 (t, $^3J(H,H) = 6$ Hz, 2H; CH_2), 8.07 (t, $^3J(H,H) = 7$ Hz, 1H; C_5H_5N), 8.14 (d, $^2J(H,H) = 8$ Hz, 1H; C_5H_5N), 8.58 (t, $^3J(H,H) = 6$ Hz, 1H; C_5H_5N), 8.99 ppm (d, $^2J(H,H) = 6$ Hz, 1H; C_5H_5N).

Synthesis of $[Zn_3Br_6\{\mu\text{-}OCH_2CH_2\text{-}NC_5H_4(4\text{-}CH_3)\}_3]$ (2c-EO): Complex **2c-EO** was prepared by reacting **1c** with ethylene oxide in methylene chloride (30 mL) at room temperature for 10 h in a 60 mL high-pressure glass reactor. After the reaction, the solution was dried under vacuum to give a white solid. Yield; 68%; elemental analysis calcd (%) for $C_{24}H_{33}Br_6N_3O_3Zn_3$: C 26.52, H 3.06, Br 44.10, N 3.87, Zn 18.00; found: C 25.82, H 3.10, N 3.79, Zn 17.83; ^1H NMR (600 MHz, [D$_6$]DMSO, 25 °C): $\delta = 2.70$ (s, 3H; CH_3), 3.93 (t, $^3J(H,H) = 5$ Hz, 2H; CH_2), 4.68 (t, $^3J(H,H) = 6$ Hz, 2H; CH_2), 8.08 (d, $^2J(H,H) = 6$ Hz, 2H; C_5H_5N), 8.94 ppm (d, $^2J(H,H) = 7$ Hz, 2H; C_5H_5N).

Reaction of CO_2 with $[Zn_2Br_4\{\mu\text{-}OCH(CH_3)CH_2\text{-}NC_5H_5\}_2]$ (3a-PO): A 60 mL high-pressure glass reactor containing solution of **2a-PO** (0.50 g, 0.66 mmol) in DMSO (10 mL) was charged with 0.5 MPa CO_2 and stored at room temperature for 3 h. The precipitate obtained was filtered, washed with CH_2Cl_2, and dried under vacuum to give a white solid (0.21 g).

Coupling reactions of epoxides and CO_2: All the coupling reactions were conducted in a 100 mL stainless-steel bomb equipped with a stirring bar and an electrical heater. The reactor was charged with the appropriate catalyst and epoxide, and pressurized with CO_2 ($\approx$ 1.4 MPa). The bomb was then heated to 100 °C with the addition of CO_2 from a reservoir tank to

0947-6539/03/0903-0684 $ 20.00+.50/0 *Chem. Eur. J.* **2003**, *9*, No. 3

Table 4. Crystallographic data for complexes **2a-PO**, **2b-PO**, **2a-EO**, **2b-EO**, and **2c-EO**.

	2a-PO	**2b-PO**	**2a-EO**	**2b-EO**	**2c-EO**
formula	$C_8H_{11}Br_2NOZn$	$C_{18}H_{26}Br_4N_2O_2Zn_2$	$C_{23}H_{31}Br_6Cl_4N_3O_3Zn_3$	$C_{26}H_{39}Br_6N_3O_4SZn_3$	$C_{27}H_{39}Br_6Cl_6N_3O_3Zn_3$
M_r	362.37	752.79	1214.88	1165.23	1341.88
crystal size [mm]	$0.46 \times 0.46 \times 0.15$	$0.40 \times 0.38 \times 0.10$	$0.42 \times 0.36 \times 0.18$	$0.25 \times 0.25 \times 0.13$	$0.41 \times 0.53 \times 0.33$
crystal system	monoclinic	monoclinic	monoclinic	monoclinic	triclinic
space group	$P2_1/c$	$P2_1/c$	$P2_1/c$	$P2_1/c$	$P\bar{1}$
a [Å]	8.869(1)	7.886(2)	7.791(2)	19.660(5)	11.188(2)
b [Å]	10.615(2)	8.594(2)	22.635(6)	10.660(3)	14.319(2)
c [Å]	13.229(3)	19.364(5)	21.693(6)	19.928(5)	15.023(3)
α [°]					68.819(2)
β [°]	104.15(2)	101.168(5)	94.005(5)	114.234(4)	74.215(3)
γ [°]					80.259(3)
V [Å^3]	1207.6(4)	1287.5(6)	3816(2)	3808.4(2)	2152.7(6)
Z	4	4	4	4	2
T [K]	293(2)	173(2)	173(2)	173(2)	173(2)
ρ_{calcd} [Mg m^{-3}]	1.993	1.942	2.115	2.032	2.070
$F(000)$	696	728	2328	2256	1296
θ range [°]	2.37–25.95	2.14–28.25	1.30–28.32	1.90–28.32	1.53–28.32
reflections collected/unique	1616/1503	7458/3030	51796/9315	22972/9126	33324/10255
R_{int}	0.0457	0.0579	0.1434	0.0538	0.0363
data/restrains/parameters	1503/0/118	3030/0/160	9315/1/403	9126/0/394	10255/0/464
GOF on F^2	1.092	1.082	0.965	1.031	1.054
final R_1, wR_2 [$I > 2\sigma(I)$]	0.0481, 0.1110	0.0604, 0.1415	0.0569, 0.1132	0.0612, 0.1371	0.0298, 0.0754
R_1, wR_2 (all data)	0.0505, 0.1126	0.1008, 0.1596	0.1309, 0.1331	0.1080, 0.1534	0.0409, 0.0786

maintain the pressure at 3.4 MPa. After the reaction, the bomb was cooled to room temperature and the remaining epoxide was removed. The product mixtures were analyzed by an Hewlett–Packard 6890 gas chromatograph equipped with a flame-ionization detector and a DB-wax column (30 m × 0.32 mm × 0.25 μm) and Hewlett–Packard 6890–5973 MSD GC-Mass spectrometer. In the case of epoxide or pyridine exchange reactions, the molar ratio of epoxide to catalyst was reduced to 10 for the NMR investigations.

CO_2 insertion reaction for IR and NMR experiments: Inside a dry box, **2a-PO** (15 mg) dissolved in [D_6]DMSO (0.5 mL) was charged into a thick-walled NMR tube (o.d.: 5 mm) equipped with a Teflon valve. The tube was pressurized with $^{13}CO_2$ (0.14 MPa) and subjected to NMR analysis. A solution of **2a-PO** (0.1 g, 0.14 mmol) in methanol (5 mL) was coated onto a 25 mm × 3 mm CaF_2 window for IR analysis. The coated window was dried and placed in a specially designed gas cell. The IR cell was charged with CO_2 (0.21 MPa) and the absorption changes were recorded with time in the carbonate region.

X-ray crystallographic studies of complexes. Data collection for the crystal structure of **2a-PO** were performed at 293 K using a CAD-4 diffractometer.[23] Details of all structure determinations are collected in Table 4. All the procedures to obtain single crystals suitable for X-ray analysis were carried out inside a dry box under an atmosphere of argon. Each complex (0.1 g) was dissolved in DMSO (7 mL) in a vial, which was contained inside a larger vial with approximately 2 mL of methylene chloride. Methylene chloride was allowed to slowly diffuse into the DMSO solution by keeping the vial at ambient temperature for several days. Crystals of **2b-PO**, **2a-EO**, **2b-EO**, and **2c-EO** with appropriate dimensions were mounted on glass fiber in random orientation. Preliminary examination and data collection were performed at 173 K by using a Siemens SMART CCD Detector single-crystal X-ray diffractometer equipped with $Mo_{K\alpha}$ radiation ($\lambda =$ 0.71073). Structure solution and refinement were carried out by using the SHELXTL-PLUS (5.1) software package (G. M. Sheldrick, Siemens Analytical X-Ray Division, Madison, WI, 1997). The non-hydrogen atoms were refined anisotropically and the hydrogen atoms were treated by using an appropriate riding model. The final residual values for the observed reflections [$I > 2\sigma(I)$] and for all reflections, and relevant structure refinement parameters are listed in Table 4. CCDC-182781 (**2b-PO**), CCDC-182779 (**2a-EO**), CCDC-182780 (**2b-EO**), CCDC-182782 (**2c-EO**) contain the supplementary crystallographic data for this paper. These data can be obtained free of charge via www.ccdc.cam.ac.uk/conts/retrieving.html (or from the Cambridge Crystallographic Data Centre, 12 Union Road, Cambridge CB21EZ, UK; fax: (+44) 1223-336-033; or e-mail: deposit@ccdc.cam.ac.uk).

Acknowledgement

This work was supported by the Ministry of Environment in Korea.

[1] A. Behr, *Carbon Dioxide Activation by Metal Complexes*, VCH, New York, **1988**.
[2] D. J. Darensbourg, M. W. Holtcamp, *Coord. Chem. Rev.* **1996**, *153*, 155–174.
[3] W. J. Peppel, *Ind. Eng. Chem.* **1958**, *50*, 767–770.
[4] M. Aresta, E. Quaranta, *CHEMTECH* **1997**, *March*, 32–40.
[5] A. G. Shaikh, *Chem. Rev.* **1996**, *96*, 951–976.
[6] J. J. Lagowski, *The Chemistry of Nonaqueous Solvents*, Academic Press, New York, **1976**.
[7] M. Inaba, Z. Siroma, A. Funabiki, M. Asano, *Langmuir* **1996**, *12*, 1535–1540.
[8] D. Ji, X. Ju, R. He, *Appl. Catal. A* **2000**, *203*, 329–333.
[9] H. Kawanami, Y. Ikushima, *Chem. Commun.* **2000**, 2089–2090.
[10] J. Gao, S. Zhong, *J. Mol. Catal. A* **2001**, *168*, 241–246.
[11] H. Matzuda, A. Niangawa, R. Nomura, *Chem. Lett.* **1979**, 1261–1262.
[12] R. Nomura, A. Ninagawa, H. Matsuda, *J. Org. Chem.* **1980**, *45*, 3735–3738.
[13] H. Kisch, R. Millini, I. J. Wang, *Chem. Ber.* **1986**, *119*, 1090–1094.
[14] W. Dümler, H. Kisch, *Chem. Ber.* **1990**, *123*, 277–283.
[15] M. Ratzenhofer, H. Kisch, *Angew. Chem.* **1980**, *92*, 303; *Angew. Chem. Int. Ed. Engl.* **1980**, *19*, 317–318
[16] K. Yamaguchi, K. Ebitani, T. Yosida, H. Yosida, K. Kaneda, *J. Am. Chem. Soc.* **1999**, *121*, 4526–4527.
[17] D. J. Darensbourg, M. W. Holtcamp, *Macromolecules* **1995**, *28*, 7577–7579.
[18] M. Cheng, E. B. Lobkovsky, G. W. Coates, *J. Am. Chem. Soc.* **1998**, *120*, 11018–11019.
[19] M. Cheng, D. R. Moor, J. J. Reczek, B. M. Chamberlain, E. B. Lobkovsky, G. W. Coates, *J. Am. Chem. Soc.* **2001**, *123*, 8738–8749.
[20] R. L. Paddock, S. T. Nguyen, *J. Am. Chem. Soc.* **2001**, *123*, 11498–11499.
[21] D. J. Darensbourg, S. A. Niezgoda, J. D. Drapper, J. H. Reibenspies, *J. Am. Chem. Soc.* **1998**, *120*, 4690–4698.
[22] D. J. Darensbourg, M. S. Zimmer, *Macromolecules* **1999**, *32*, 2137–2140.

  0947-6539/03/0903-0685 $ 20.00+.50/0

[23] H. S. Kim, J. J. Kim, B. G. Lee, O. S. Jung, H. G. Jang, S. O. Kang, *Angew. Chem.* **112**, 4262 – 4264; *Angew. Chem. Int. Ed.* **2000**, *39*, 4096 – 4097.
[24] P. A. van der Schaaf, E. Wissing, J. Boersma, W. J. J. Smeets, A. L. Spek, G. van Koten, *Organometallics*, **1993**, *12*, 3624 – 3629.
[25] F. H. van der Steen, J. Boersma, A. L. Spek, G. van Koten, *Organometallics* **1991**, *10*, 2467 – 2480.
[26] M. M. Olmstead, P. P. Power, S. C. Shoner, *J. Am. Chem. Soc.* **1991**, *113*, 3379 – 3385.
[27] D. J. Darensbourg, S. A. Niezgoda, J. D. Draper, J. H. Reibenspies, *Inorg. Chem.* **1999**, *38*, 1356 – 1359.
[28] M. Kunert, M. Brauer, O. Klobes, H. Gorls, E. Dinjus, E. Anders, *Eur. J. Inorg. Chem.* **2000**, 1803 – 1809.
[29] D. J. Darensbourg, J. R. Wildeson, J. C. Yargrough, J. H. Reibenspies, *J. Am. Chem. Soc*. **2000**, *122*, 12 487 – 12 496.
[30] M. Tokunaga, J. F. Larrow, F. Kakiuchi, E. N. Jacobsen, *Science* **1997**, *277*, 936 – 938.
[31] S. E. Schaus, E. N. Jacobsen, *Tetrahedron Lett.* **1996**, *37*, 7937 – 7940.
[32] M. Kato, T. Ito, *Inorg. Chem.* **1985**, *24*, 509 – 514.
[33] D. J. Darensbourg, M. W. Holtcamp, G. E. Struck, M. S. Zimmer, S. A. Niezgoda, P. Rainey, J. B. Robertson, J. D. Draper, J. H. Reibenspies, *J. Am. Chem. Soc*. **1999**, *121*, 107 – 116.
[34] K. Nakamoto, *Infrared and Raman Spectra of Inorganic and Coordination Compounds*, Wiley, New York, **1997**.
[35] M. Kato, T. Ito, *Inorg. Chem.* **1985**, *24*, 504 – 508.
[36] C. Postmus, J. R. Ferraqo, W. Wozniak, *Inorg. Chem.* **1967**, *6*, 2030 – 2032.

Received: April 4, 2002
Revised: September 4, 2002 [F3997]

  0947-6539/03/0903-0686 $ 20.00+.50/0